Constant Envelope MIMO-OFDM Precoding for Low Complexity Large-Scale Antenna Array Systems

Stavros Domouchtsidis, *Student Member, IEEE*, Christos G. Tsinos, *Senior Member, IEEE*, Symeon Chatzinotas, *Senior Member, IEEE*, and Björn Ottersten, *Fellow, IEEE*

***Abstract*— Herein, we consider constant envelope precoding in a multiple-input multiple-output orthogonal frequency division multiplexing system (CE MIMO-OFDM) for frequency selective channels. In CE precoding the signals for each transmit antenna are designed to have constant amplitude regardless of the channel realization and the information symbols that must be conveyed to the users. This facilitates the use of power-efficient components, such as phase shifters (PS) and nonlinear power amplifiers, which are key for the feasibility of large-scale antenna array systems because of their low cost and power consumption. The CE precoding problem is firstly formulated as a least-squares problem with a unit modulus constraint and solved using an algorithm based on coordinate descent. The large number of optimization variables in the case of the MIMO-OFDM system motivates the search for a more computationally efficient solution. To tackle this, we reformulate the CE precoding design into an unconstrained nonlinear least-squares problem, which is solved efficiently using the Gauss-Newton algorithm. Simulation results underline the efficiency of the proposed solutions and show that they outperform state of the art techniques.**

***Index Terms*— Constant-envelope precoding, low-PAR precoding, large MIMO, multi-user, MIMO-OFDM.**

I. Introduction

THE use of large-scale antennas at the base station (BS) is crucial for the future of wireless communications, as they have shown to offer much needed improvements in average spectral as well as energy efficiency, [3]– [5]. In such systems, antenna arrays with tens or hundreds of elements are used to communicate with multiple user terminals (UTs) over the same time and frequency resource block. To mitigate the induced multiuser interference (MUI), which has a degrading effect on the performance of the system, precoding techniques have to be employed.

Manuscript received May 14, 2019; revised March 24, 2020 and July 30, 2020; accepted August 10, 2020. Date of publication August 27, 2020; date of current version December 10, 2020. This work was supported by the Fonds National de la Recherche (FNR), Luxembourg, under the CORE Projects Efficient Millimeter-Wave Large-Array Communications (ECLECTIC) and INTER CI-PHY. This article was presented at the ICASSP. The associate editor coordinating the review of this article and approving it for publication was N. Prasad. *(Corresponding author: Stavros Domouchtsidis.)*

The authors are with the Interdisciplinary Centre for Security, Reliability, and Trust (SnT), University of Luxembourg, L-1855 Luxembourg City, Luxembourg (e-mail: stavros.domouchtsidis@uni.lu; christos.tsinos@uni.lu; symeon.chatzinotas@uni.lu; bjorn.ottersten@uni.lu).

Color versions of one or more of the figures in this article are available online at https://ieeexplore.ieee.org.

Digital Object Identifier 10.1109/TWC.2020.3018431

There is a large number of works in the literature that propose various precoding techniques and can be classified in two main categories depending on the information that they use in order to construct the precoder [6]. In the first category of block-level precoding (BLP) we have precoding techniques that use only the channel state information (CSI), such as the ones proposed in [13]– [15] and therefore the precoder needs to be updated only when the channel changes. The second category includes techniques that utilize both the CSI as well as the information symbols that should be conveyed to the users in order to construct the precoder. Because, these precoders depend on the transmitted symbols, they need to be updated on a symbol rate. For this reason, this category of precoding techniques is named symbol level precoding (SLP), [7]– [12]. The main disadvantage of SLP is its increased complexity, since the precoder has to be updated on a symbol rate. For this reason, its use is suggested at the BS which is usually equipped with capable hardware that can complete the SLP design on a real-time basis.

Most of the SLP techniques in the literature do not necessarily have the objective to reduce the MUI but rather turn it into constructive interference by pushing the received symbols at the UTs further into the decision regions, [10]. These techniques usually require transmitter architectures where the signal processing is entirely implemented in the baseband domain and therefore a dedicated digital to analog converter (DAC) is required for each antenna. Furthermore, after the digital to analog conversion they require the use of highly linear RF components such as power amplifiers, which tend to have a low power-efficiency.

The problem with these power-inefficient components becomes more noticeable in large-scale antenna arrays where tens or hundreds of these components have to be used. Additionally, large arrays are usually equipped with amplifiers that are easier to saturate because the gain is expected to come from beamforming. For this reason, the feasibility of these systems depends on the use of more power efficient components and therefore the development of precoding techniques that produce transmit signals that allow the use of power-efficient components. In the literature, there are already, techniques which fall into the SLP category such as constant envelope (CE) precoding, [26]– [30], or RF domain SLP, [20], that design the transmit signal to facilitate the use of power-efficient and low cost components. In CE precoding the

amplitude of the discrete time signal that is transmitted by each BS antenna remains constant regardless of the channel realization or the information symbols that are conveyed to the users. As a result these transmit signals have low peak-to-average ratio (PAR) and make possible the use of power efficient nonlinear power amplifiers. In RF domain SLP [20], the transmit signal is designed so that the processing occurs in the RF domain, eliminating the use for DACs.

The CE precoding work was extended in [2] to include CE single-carrier transmission over frequency selective channels and later it was shown in [1] that the same algorithm, presented in [2], can be used for OFDM transmission if we precode the inverse Fourier transform of the information symbols rather than the information symbols themselves. The processing occurs in the time domain and therefore the iterative solution includes the computation of the convolution at each iteration which leads to a high computational complexity.

In this paper we present a novel way to tackle the problem of CE precoding for MIMO-OFDM transmission over a frequency selective channel. By rewriting the CE constraint in the frequency domain, in a similar way to [31], we reformulate the design problem. This enables an efficient solution by minimizing the Euclidean distance between the Fourier Transform of the received signal and the desired information symbols.

- First, we employ a mathematical formulation of the MIMO-OFDM system, similar to the one proposed in [31], that enables the development of efficient algorithmic solutions. The aim of the formulation is to directly design in a nonlinear manner the time domain signal of the OFDM system such that to be of constant amplitude (CE). The improved efficiency is the result of eliminating the need for the computation of the convolution of the multipath channel with the transmit signal during the search of the solution, as required in current state of the art solutions.
- We propose the use of power efficient transmitter architectures for CE MIMO-OFDM precoding, that utilize analog phase shifters and nonlinear power amplifiers and we develop an efficient algorithmic framework to solve the precoding problem when such architectures are used. Additionally, we derive the power consumption model of these architectures for the case where CE MIMO-OFDM precoding is used.
- We propose the use of a post-processing scalar factor which changes on a per OFDM block basis, and partially compensates for the lack of amplitude control in the transmitter because of CE precoding. This scalar factor facilitates the exploitation of the array gain provided by the large-scale antenna array by scaling the signal at the receivers accordingly. We propose a blind estimation of the scalar that exploits the block structure of OFDM transmission and does not introduce communication overhead or delay in the demodulation process, as would happen in single carrier systems.
- We then formulate the CE precoding problem as a least-squares problem with a unit modulus constraint and we solve it using an algorithm based on Coordinate Descent (CD).
- Finally, we propose a second more efficient solution using the Gauss-Newton (GN) algorithm by reformulating the problem into an unconstrained nonlinear least-squares problem.

The remainder of the paper is structured as follows. In Section II the system model of a classic MIMO-OFDM system is presented followed by the description of the system model of CE MIMO-OFDM and the formulation of the CE MIMO-OFDM precoding problem. The section ends by a presentation of power-efficient transmitter architectures for CE MIMO-OFDM precoding. In Section III, we present two different solution for the precoding problem, first a solution based on CD and then a solution using the GN method. In Section IV we present numerical results of simulations of the proposed system and we compare it with Zero Forcing precoding and CE techniques from the literature ([1], [2]), showing the advantages that our solutions provide. Finally, in Section V we discuss the conclusions of this work.

Notations: $\imath$ denotes the imaginary unit, $||\cdot||_F$ denotes the Frobenius norm, $||\cdot||_2$ denotes the L-2 norm, $E[\cdot]$ denotes the expectation operator, $\mathbb{R}$ denotes the set of real numbers, $\Re$ denotes the real part of a complex number, $\Im$ denotes the imaginary part of a complex number, $[\cdot]^T$ denotes the transpose of a matrix and $[\cdot]^H$ denotes the conjugate transpose of a matrix.

II. System Model

Before we describe the system model of the proposed CE MIMO-OFDM scheme, let us first briefly consider the downlink of a classic multiuser MIMO-OFDM, using a linear precoding scheme (i.e. Zero Forcing precoding), system operating over a frequency selective channel.

A. MIMO-OFDM

In the considered wireless communication system we have a BS equipped with a large array of M antennas serving K single-antenna UTs over a bandwidth W using OFDM.

Generally in OFDM, the channel, of bandwidth W, that is assigned for transmission is divided into N sub-channels with equal width of $\Delta f = W/N$, because it is assumed that a signal of bandwidth W will suffer from frequency selective fading as a result of the multipath propagation. The width Δf of the sub-channels is chosen so that it will be smaller than the coherence bandwidth of the channel so that the frequency response of the channel will be flat over each sub-channel. Each sub-carrier that corresponds to one of the N sub-channels is modulated forming the $M \times N$ OFDM block in the frequency domain

$$\mathbf{X}_F = [\mathbf{x}_F(1),\ \mathbf{x}_F(2),\ \ldots,\ \mathbf{x}_F(N)]\,, \tag{1}$$

where $\mathbf{x}_F(n)$ is an $M \times 1$ column vector that is loaded on the n_{th} sub-carrier and which contains the M precoded symbols, one for each transmit antenna of the BS.

In order to produce the OFDM signal in the time domain the N-point inverse FFT (IFFT) is applied on each row of the

frequency domain signal $\mathbf{X}_F$ and the result is the time domain signal

$$\mathbf{X}_T = \sqrt{N}\ \text{IFFT}(\mathbf{X}_F, 2) = \left(\frac{\mathbf{W}^*}{\sqrt{N}}\mathbf{X}_F^T\right)^T, \quad (2)$$

where IFFT$(\cdot, 2)$ denotes the row wise IFFT and $\mathbf{W}_N$ is the $N \times N$ Discrete Fourier Transform (DFT) matrix.

After the IFFT computation, the Cyclic Prefix is added at the beginning of the OFDM block $\mathbf{X}_T$. The CP has a length, which must be larger or at least equal to the multipath channel's length, of L samples, and is comprised by the last L samples of $\mathbf{X}_T$,

$$\mathbf{CP} = [\mathbf{x}_T(N-L+1),\ \ldots,\ \mathbf{x}_T(N-1),\ \mathbf{x}_T(N)], \quad (3)$$

where $\mathbf{x}_T(n)$, is the n-th $M \times 1$ column of $\mathbf{X}_T$, and represents the n-th time domain symbol which is transmitted from the M transmit antennas.

After prepending the cyclic prefix the signal is transmitted over a channel with ν resolvable multipath components which is expressed as

$$\mathbf{h}_T(m,k) = [h(m,k,1),\ h(m,k,2),\ \ldots.\ h(m,k,\nu)], \quad (4)$$

where $h(m,k,n)$ is the n-th path gain from the m-th transmit antenna of the BS to the k-th UT. Additionally, in the scope of this paper we assume Rayleigh fading and therefore the channel coefficients are modelled as circularly symmetric complex Gaussian random variables with $h(m,k,n) \sim \mathcal{CN}(0, \frac{1}{\nu})$. The received time domain signal at the k-th receiver is denoted by

$$y_T(k,n) = \sum_{m=1}^{M}\sum_{l=0}^{v-1} h(m,k,l)x_T(m,n-l) + z_T(k,n), \quad (5)$$

where $z_T(k,n)$ is the n-th noise sample which is modelled as a circularly symmetric complex Gaussian random variable with distribution $z_T(k,n) \sim \mathcal{CN}(0, N_0)$, where N_0 is the noise variance. Additionally, in the scope of this paper it is assumed that the CSI is constant for some interval long enough for the transmitter to learn and use it until it changes to a new value and therefore, the proposed scheme should be employed in applications that this assumption is valid.

The k-th receiver performs an FFT on the received signal after removing the CP which is equivalent to discarding the first L samples of $\mathbf{y}_T(k)$. The output of the N point FFT at the k-th UT is given by

$$y_F(k,n) = \sum_{m=1}^{M} h_F(k,m,n)x_F(m,n) + z_F(k,n), \quad (6)$$

with $n = 1, 2, \ldots, N$ where $h_F(m,k,n)$ and $z_F(k,n)$ are the frequency domain channel coefficients and AWGN noise samples, respectively. Finally, a simple detector, based on nearest neighbour search, is employed in order to detect the information symbols that have been transmitted.

B. CE MIMO-OFDM

Now that we have a basic understanding of the MIMO-OFDM system let us continue with the CE MIMO-OFDM. Here the transmit signal in the time domain is constrained to have a per antenna constant amplitude regardless of the transmitted symbols and channel realization, which is expressed by

$$|x_T(m,n)| = \sqrt{\frac{\gamma}{M}} \quad (7)$$

where $\frac{\gamma}{M}$ is the per antenna constant power constraint and γ is the total transmit power. The problem with (7) is that it constrains the signal in the time domain and there is not an easy way to transform the constraint in the frequency domain where the processing happens in OFDM transmission.

Before we formulate the CE MIMO-OFDM precoding problem, it is important to show how the frequency domain channel coefficients are formulated appropriately into a $KN \times MN$ matrix $\tilde{\mathbf{H}}_F$, the DFT matrix $\mathbf{W}_N$ into a $MN \times MN$ matrix $\tilde{\mathbf{W}}_N$ that helps us compute the N-point DFT of a $MN \times 1$ vector $\tilde{\mathbf{x}}_T$, which is comprised not only from symbols of different time slots but also of different antennas and it is structured as

$$\tilde{\mathbf{x}}_T = \begin{bmatrix} \mathbf{x}_T(1) \\ \mathbf{x}_T(2) \\ \vdots \\ \mathbf{x}_T(N) \end{bmatrix},$$

where $\mathbf{x}_T(n)$, is an $M \times 1$ vector, and represents the n-th time domain sample which is transmitted from the M transmit antennas. In other words, $\tilde{\mathbf{x}}_T$ is $\mathbf{X}_T$ written in a vector form.

Now we will show how to reshape the frequency selective MIMO channel as a $KN \times MN$ block matrix as

$$\tilde{\mathbf{H}}_F = \begin{bmatrix} \tilde{\mathbf{H}}_{F1} & 0 & \ldots & 0 \\ 0 & \tilde{\mathbf{H}}_{F2} & \ldots & 0 \\ \vdots & \vdots & \ddots & \vdots \\ 0 & 0 & \ldots & \tilde{\mathbf{H}}_{FN} \end{bmatrix},$$

where $\tilde{\mathbf{H}}_{Fn}$ is a $K \times M$ matrix that denotes the channel frequency response over the n-th sub-carrier, with $n = 1, 2, \ldots, N$ and its elements $\tilde{H}_{Fn}(k,m)$ denoting the fading coefficient from the m-th transmit antenna to the k-th UT.

Finally, we will show how to construct the DFT matrix $\tilde{\mathbf{W}}_N$ that can be used to compute the N-point DFT by multiplying it with $\tilde{\mathbf{x}}_T$. This matrix is the Kronecker product, $\tilde{\mathbf{W}}_N = \mathbf{W}_N \otimes \mathbf{I}_M$ defined as

$$\tilde{\mathbf{W}}_N = \begin{bmatrix} W_N(1,1)\mathbf{I}_M & W_N(1,2)\mathbf{I}_M & \ldots & W_N(1,N)\mathbf{I}_M \\ W_N(2,1)\mathbf{I}_M & W_N(2,2)\mathbf{I}_M & \ldots & W_N(2,N)\mathbf{I}_M \\ \vdots & \vdots & \ddots & \vdots \\ W_N(N,1)\mathbf{I}_M & W_N(N,2)\mathbf{I}_M & \ldots & W_N(N,N)\mathbf{I}_M \end{bmatrix},$$

where $\mathbf{I}_M$ is the $M \times M$ identity matrix.

The problem of minimizing the MUI across all users in CE precoding MIMO-OFDM can now be formulated as a constrained least squares problem,

$$(\mathcal{P}_1):\ \min_{\tilde{\mathbf{x}}_T, \beta} ||\tilde{\mathbf{s}} - \beta\tilde{\mathbf{H}}_F\tilde{\mathbf{W}}_N\tilde{\mathbf{x}}_T||_2^2 \quad (8)$$

$$s.t.\ |\tilde{\mathbf{x}}_T(m)| = \sqrt{\frac{\gamma}{M}} \quad m = 1, \ldots, MN \quad (9)$$

$$\text{and } \beta \in \mathbb{R}, \quad (10)$$

where $\tilde{\mathbf{s}}$ is an $KN \times 1$ vector containing the information symbols that must be conveyed to the K UTs over the N sub-carriers. The N information symbols corresponding to the k-th UT are drawn from a constellation which is assumed to have average power equal to the target received power for this UT. Here we also introduce β, a scalar which is applied at the receivers, and allows us to exploit the array gain of the multiple transmit antennas of the BS, and depends on the transmitted symbols and the channel realization [16]. This factor remains constant for the whole OFDM block in order to enable its blind estimation at the UTs. Additionally, it is kept common across all users in order to decrease the computational complexity and achieve performance fairness among the UTs.

The problem formulation $\mathcal{P}_1$ means that we are looking for the vector $\tilde{\mathbf{x}}_T$ with elements of constant amplitude equal to $\sqrt{\gamma/M}$, as well as the factor β that minimize the distance between the vector of information symbols $\tilde{\mathbf{s}}$ and the FFT of the received noiseless signal $\tilde{\mathbf{H}}_F\tilde{\mathbf{W}}\tilde{\mathbf{x}}_T$. Additionally, it is assumed that the UTs rescale the received signal by β before estimating the conveyed information symbols. The choice to address the case of the noiseless received signals was made in order to achieve a solution that is as computationally efficient as possible since the problem of CE MIMO-OFDM is already a hard problem to tackle.

Once the optimal vector $\tilde{\mathbf{x}}_{opt,T}$ is computed, the IFFT does not have to be computed as in classic OFDM because our signal is already in the time domain. However we still have to prepend the cyclic prefix with length of LM samples at the beginning of $\tilde{\mathbf{x}}_{opt,T}$. After that, the signal is transmitted by loading to the M antennas during the n-th time slot the symbols $[\tilde{\mathbf{x}}_{opt,T}((n-1)M+1),\ \tilde{\mathbf{x}}_{opt,T}((n-1)M+2),\ \ldots,\ \tilde{\mathbf{x}}_{opt,T}(nM)]$.

At each UT, after the removal of the first L samples of the received signal which correspond to the cyclic prefix, the N-point FFT of the received signal is computed. If we concatenate the outputs of the FFT from all the UTs we get

$$\tilde{\mathbf{y}}_F = \tilde{\mathbf{H}}_F\tilde{\mathbf{W}}_N\tilde{\mathbf{x}}_T + \tilde{\mathbf{z}}_F \tag{11}$$

where $\tilde{\mathbf{y}}_F$ is a $KN\times 1$ vector and $\tilde{\mathbf{z}}_F$ a $KN\times 1$ vector formed by the noise samples in the frequency domain. Each receiver must estimate the factor β and scale the signal accordingly before making a decision on the transmitted symbols. The factor can be estimated blindly or using pilot symbols as it was proposed in [16]. Here we estimate $\hat{\beta}_k$ blindly at the receiver according to the equation

$$\hat{\beta}_k = \sqrt{\frac{||\mathcal{Q}||^2/M_Q + N_0}{||\mathbf{y}_F^{(k)}||^2/N}}, \tag{12}$$

where $\mathcal{Q}$ is the employed constellation, M_Q is the order of the constellation and $\mathbf{y}_F^{(k)}$ is the $N \times 1$ output of the FFT at the k-th receiver. It should be noted that although β is common for all UTs, the estimated $\hat{\beta}_k$ may have small variations among the UTs since each UT uses only $\mathbf{y}_F^{(k)}$ to estimate it. Finally, each UT employs a simple nearest neighbour type detector on the scaled signal $\hat{\beta}_k\mathbf{y}_F^{(k)}$ to estimate the symbols that have been sent.

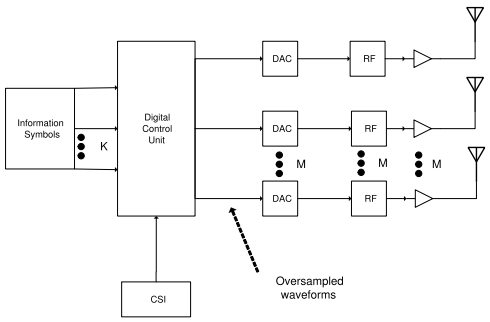

Fig. 1. Block diagram of the CE MIMO-OFDM transmitter with a DAC per antenna.

C. CE Transmitter Architecture

In a transmitter operating with a conventional precoder, such as a Zero-Forcing precoder, the large envelope fluctuations of the signal would lead to significant nonlinear distortions by the power amplifiers. In order to mitigate the distortion, each amplifier has to work in its linear region, but this leads to a low power efficiency, [21]. On the other hand, a system that uses CE signals such as the one that we propose in this paper is not affected by the distortions produced by amplitude nonlinearities when appropriate filtering is used, [33].

In order to quantify the effects of the power amplifier on the transmitted signal we are going to use the model for a solid state power amplifier (SSPA) presented in [21]– [22], in which the time domain envelope response also referred to as AM/AM characteristic is given by

$$g(A) = A_{o,max}\frac{A/A_{max}}{\left[1+(A/A_{max})^{2p}\right]^{\frac{1}{2p}}}, \tag{13}$$

where A is the envelope of the input signal given by

$$A = |\tilde{\mathbf{x}}_T|, \tag{14}$$

$A_{o.max}$ is the maximum amplitude of the output signal given by

$$A_{o,max} = \upsilon A_{max}, \tag{15}$$

with υ denoting the signal gain of the amplifier and A_{max} is the input reference amplitude. Finally, p is a positive parameter that controls the smoothness of the transition from the linear region to the limiting region. According to [21] the AM/PM conversion of an SSPA is assumed to be very small and therefore can be neglected.

The average power amplifier efficiency of such an amplifier, according to [22], is given by

$$\eta = \frac{\pi}{4}\frac{E[A_o^2]}{A_{o,max}E[A_o]}, \tag{16}$$

where A_o is the envelope of the output signal.

A classic large-scale antenna array BS would require a dedicated RF chain and DAC for each transmit antenna, as it is shown in Fig.1, which makes the system very inefficient as the power consumption greatly increases when a large-scale antenna with hundreds of elements is used. The proposed per antenna CE precoding means that we can reduce the

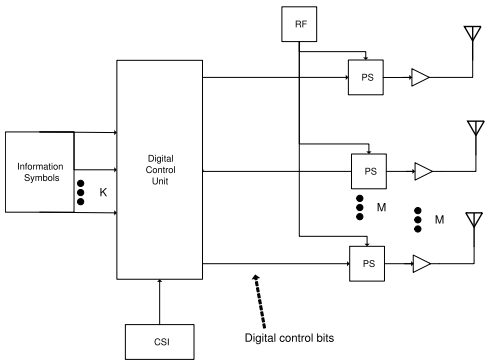

Fig. 2. Block diagram of the CE MIMO-OFDM transmitter with 1-PS per antenna.

power consumption of the transmitter because it facilitates the operation of the PAs in their nonlinear region where they are more power efficient. However, there can be further gains in power efficiency if we make alterations to the transmitter's architecture that fully exploit the CE nature of the signal.

The proposed system transmits signals from each antenna that do not change in amplitude but only in phase, since the CE signal can be written as

$$\tilde{\mathbf{x}}_T = \sqrt{\frac{\gamma}{M}} e^{\imath\tilde{\theta}}, \tag{17}$$

where $\tilde{\theta}$ is an $MN \times 1$ vector which contains the phase shifts of the transmit signal for one OFDM block of N sub-carriers across the M transmit antennas of the BS. Additionally, contrary to classic OFDM systems where each sub-carrier is modulated separately before computing the IFFT, here the CE time domain signal is computed in a digital processing unit so that the N-point FFT at each UT will be as close as possible to the information symbols that we want to convey. Therefore, it is not necessary to use a DAC at each transmit antenna, which would consume power, to produce the baseband signal. Motivated by these reasons, we propose to use in place of the M DACs, M digitally controlled PSs as shown in Fig.2, which will alter the phase of the sinusoidal carrier wave according to $\tilde{\theta}$ at each antenna in order to produce the transmit signal $\tilde{\mathbf{x}}_T$.

To underline the gains from using PSs to modulate the RF signal instead of DACs we will give the approximation of the power consumption of a transmitter utilizing DACs and of one utilizing PSs, using the models developed in [17]– [20]. The consumed power of the fully digital architectures shown in Fig.1 is given by

$$P_{FD} = \frac{E[||\tilde{\mathbf{x}}_T||_2^2]}{\eta} + M(P_{DAC} + P_{LO} + P_{mix} + P_{fil}), \tag{18}$$

where P_{DAC}, P_{LO}, P_{mix}, P_{fil} is the power consumed by a DAC, a local oscillator, a mixer, and a filter of the transmitter respectively, while the consumed power of the CE transmitter that uses PSs shown in Fig.2 is given by

$$P_{RF-CE} = \frac{E[||\tilde{\mathbf{x}}_T||_2^2]}{\eta} + M(P_{PS} + P_{LO} + P_{mix} + P_{fil}), \tag{19}$$

Algorithm 1 CD CE MIMO-OFDM

Input: $\tilde{\mathbf{Q}}$, $\tilde{\mathbf{s}}$
Initialize β, $\tilde{\mathbf{x}}_T$
while $\left|\beta^{(n)} - \beta^{(n-1)}\right| \leq \epsilon_1$ **do**
  while $\left|\tilde{\mathbf{x}}_T(j) - \tilde{\mathbf{x}}_T^{(j-1)}\right| \leq \epsilon_2$ **do**
    for $i = 1$ to MN **do**
      Update x_{Ti}, according to (23)
    end for
  end while
  Update the value of β, according to (25)
end while
Output: $\tilde{\mathbf{x}}_T$, β

where P_{PS} is the power consumed by a phase shifter. Since the consumed power by the PSs is significantly smaller than the one by the DACs the gains become very significant as the number of transmit antennas M increase.

III. CE MIMO-OFDM Precoding Design

In this section we present two iterative algorithms for solving the precoding problem $(\mathcal{P}_1)$. The first is an alternating minimization algorithm based on CD. In the following subsection we will reformulate the problem $(\mathcal{P}_1)$ as an unconstrained nonlinear least-squares problem and solve it using the Gauss-Newton algorithm.

A. Coordinate Descent

CD is an easily implementable and efficient method where the cost function is minimized at each iteration over one coordinate direction [23] and CD based methods have been successfully used in the past to solve similar type optimization problems, [20]. This practically means that when we minimize over the i-th coordinate, $\tilde{x}_{Ti}$, the rest, $\tilde{x}_{Tr}$ for $r \neq i$, are kept fixed to their previous values. As a result a full iteration of CD includes as many sub-iterations as the number of coordinates, in our problem MN. Additionally, apart from minimizing the cost function of $(\mathcal{P}_1)$ over $\tilde{\mathbf{x}}_T$ we also have the factor β, and therefore we have to resort to alternating optimization. Finally, before we move on with a more detailed explanation of the iterative solution, let us slightly reformulate $(\mathcal{P}_1)$ by replacing the matrix multiplication in the cost function with an equivalent $KN \times MN$ matrix $\tilde{\mathbf{Q}} = \tilde{\mathbf{H}}_F \tilde{\mathbf{W}}_N$ we obtain

$$(\mathcal{P}_2): \min_{\tilde{\mathbf{x}}_T, \beta} ||\tilde{\mathbf{s}} - \beta\tilde{\mathbf{Q}}\tilde{\mathbf{x}}_T||_2^2 \tag{20}$$

$$s.t.\ |\tilde{\mathbf{x}}_{\mathbf{T}m}| = \sqrt{\frac{\gamma}{M}} \quad m = 1, \ldots, MN \tag{21}$$

$$\text{and } \beta \in \mathbb{R}. \tag{22}$$

Algorithm 1 presents the CD based solution in pseudocode. The algorithm is initialized by providing as inputs $\tilde{\mathbf{Q}}$ and the vector of information symbols $\tilde{\mathbf{s}}$ that must be conveyed to the UT. The algorithm at the i-th sub-iteration minimizes the objective function over $\tilde{x}_{Ti}$ while keeping all the other

coordinates, including β, fixed. This results to the update step

$$\tilde{x}_{Ti} = \Pr\left(\frac{\beta\tilde{\mathbf{Q}}_{\mathbf{i}}{}^{H}(\tilde{\mathbf{s}} - \beta\tilde{\mathbf{Q}}_{-i}\tilde{\mathbf{x}}_{\mathbf{T}-i})}{\beta\tilde{\mathbf{Q}}_{i}^{H}\beta\tilde{\mathbf{Q}}_{i}}\right), \tag{23}$$

where $\tilde{\mathbf{Q}}_i$ is the i-th column of $\tilde{\mathbf{Q}}$, $\tilde{\mathbf{x}}_{\mathbf{T}-i}$ is the vector produced after removing the i-th element of $\tilde{\mathbf{x}}_T$, $\tilde{\mathbf{Q}}_{-i}$ is the matrix produced after removing the i-th column of $\tilde{\mathbf{Q}}$ and $\Pr(u)$ is the projection of u onto the circle with radius $\sqrt{\gamma/M}$ given by

$$Pr\,(u) = \begin{cases} u & |u| = 0 \\ \sqrt{\dfrac{\gamma}{M}}\dfrac{u}{|u|} & |u| \neq 0. \end{cases}$$

The convergence criterion for $\tilde{\mathbf{x}}_T$ is

$$\left|\tilde{\mathbf{x}}_T^{(j)} - \tilde{\mathbf{x}}_T^{(j-1)}\right| \leq \epsilon_2, \tag{24}$$

where $\tilde{\mathbf{x}}_T^{(j)}$ is the result of the j-th update and ϵ_2 is a predefined tolerance. After this criterion is met the algorithm moves to minimize the objective function over β which results to the update step

$$\beta = \frac{\Re\{\tilde{\mathbf{s}}^H\tilde{\mathbf{Q}}\tilde{\mathbf{x}}_T\}}{||\tilde{\mathbf{Q}}\tilde{\mathbf{x}}_T||_2^2}. \tag{25}$$

Following the update of β the CD algorithm repeats the same update steps until the termination criterion, which is defined as

$$\left|\beta^{(n)} - \beta^{(n-1)}\right| \leq \epsilon_1, \tag{26}$$

is reached. Then, the algorithm outputs the optimal $\tilde{\mathbf{x}}_{opt,T}$ which is of constant amplitude equal to $\sqrt{\gamma/M}$ and β. The transmitter has no further use for β, since the UTs will blindly estimate it using (12) before detecting the transmitted symbols.

Finally, $\tilde{\mathbf{x}}_T$ has to be converted from a single $MN \times 1$ column to N parallel $M \times 1$ vectors corresponding to the N time slots of the OFDM block. As a result at the n-th time slot the signal

$$\begin{bmatrix} \tilde{x}_T((n-1)M+1) \\ \tilde{x}_T((n-1)M+2) \\ \vdots \\ \tilde{x}_T((n-1)M+M) \end{bmatrix}$$

is transmitted from the M antennas of the BS. In case the transmitter uses digitally controlled analog phase shifters, as in Fig.1 then we need the phase shifts that the PSs will impose on the RF signal. These angles can be easily extracted from $\tilde{\mathbf{x}}_T$ by calculating

$$\tilde{\theta} = \text{Arg}(\tilde{\mathbf{x}}_T), \tag{27}$$

where Arg is the principal value of a complex number.

The problem $(\mathcal{P}_2)$ that is tackled here is nonconvex and therefore the solutions are not guaranteed to be optimal. However, as the numerical results show in section V. the solution is sufficient for reliable communications as it reduces sufficiently the average MUI energy, and achieves low SER.

Finally, let us briefly discuss the computational complexity of the proposed CD based algorithm. In order to estimate the complexity of the proposed solution, we computed the number of FLOPS (floating point operations per second) per iteration of the algorithm as a function of the size of the matrices and vectors that are involved. The computational complexity in FLOPS of an iteration which updates one coordinate is given by

$$C_{CE,CDperiter} = 4KN^2M + 8KN + 6, \tag{28}$$

or in big $\mathcal{O}$ notation, $\mathcal{O}(KN^2\ M)$. However, in order to update all the coordinates the CD algorithm needs to perform MN updates. Therefore for a full iteration of the algorithm, the complexity is given by

$$C_{CE,CD} = MN(4KN^2M + 8KN + 6), \tag{29}$$

or in big $\mathcal{O}$ notation, $\mathcal{O}(KN^3\ M^2)$. The computation costs that we used to calculate the expressions above can be found in [34]. While we have observed that the algorithm converges after a few dozens of full iterations, a theoretical analysis of its convergence is an open problem. Even for cases where the addressed problem is convex [23] the convergence analysis is extremely challenging. Therefore, the convergence analysis of the nonconvex problem that we are tackling here cannot be addressed within the scope of this work.

Algorithm 2 GN CE MIMO-OFDM

1: **Input:** $\tilde{\mathbf{Q}}$, $\tilde{\mathbf{s}}$
2: **Initialize** $\mathbf{v}$
3: **while** $\left|\mathbf{v}^{(j)} - \mathbf{v}^{(j-1)}\right| \leq \epsilon$ or $j \leq$ maxIter **do**
4: Calculate $\mathbf{r}(\mathbf{v}^{(j-1)})$, according to (38)
5: Calculate $\mathbf{J}_r(\mathbf{v}^{(j-1)})$, according to (39)
6: Calculate $\mathbf{v}^{(j)}$, according to (36)
7: **end while**
8: **Output:** $\mathbf{v}$

B. Gauss-Newton

The proposed CD based method becomes computationally inefficient as the number of sub-carriers and the number of antennas increases, as (29) shows. As a reminder, a full iteration of the algorithm proposed in the previous section consists of MN, the number of optimization variables, sub-iterations and therefore an increase in the number of sub-carriers or antennas by ΔN or ΔM translates to $M\Delta N$ and $M\Delta M$ respectively, increase of sub-iterations in each full iteration. Here we show how to reformulate the problem $(\mathcal{P}_2)$ into an unconstrained nonlinear least squares problem and solve it using the simple and efficient Gauss-Newton (GN) method. GN minimizes a sum of squared functions and does so in a computational efficient way because it does not require the analytic expression for the Hessian matrix as other competing iterative methods [24]. Additionally, it has a quadratic convergence when the initial guess is relatively close to the optimal value [25].

The CE transmit signal in (17) can also be written as

$$\tilde{\mathbf{x}}_T = \sqrt{\frac{\gamma}{M}}(\cos\tilde{\theta} + \imath\sin\tilde{\theta}). \tag{30}$$

As a result we can rewrite $\mathcal{P}_3$ as

$$(\mathcal{P}_3): \quad \min_{\mathbf{v}} ||\tilde{\mathbf{s}} - \beta\tilde{\mathbf{Q}}\sqrt{\frac{\gamma}{M}}(\cos\tilde{\theta} + \imath\sin\tilde{\theta})||_2^2, \tag{31}$$

where $\mathbf{v} = [\tilde{\theta}^T \ \beta]^T$. Finally, we need to get rid of the imaginary unit and for that reason we define the residual vector $\mathbf{r}(\mathbf{v})$, $2KN \times 1$, by separating the real and imaginary parts of the cost function of $(\mathcal{P}_3)$ as

$$\mathbf{r}(\mathbf{v}) = \begin{bmatrix} \Re\{\tilde{\mathbf{s}}\} - \beta\sqrt{\frac{\gamma}{M}}(\Re\{\tilde{\mathbf{Q}}\}\cos\tilde{\theta} - \Im\{\tilde{\mathbf{Q}}\}\sin\tilde{\theta}) \\ \Im\{\tilde{\mathbf{s}}\} - \beta\sqrt{\frac{\gamma}{M}}(\Re\{\tilde{\mathbf{Q}}\}\sin\tilde{\theta} + \Im\{\tilde{\mathbf{Q}}\}\cos\tilde{\theta}) \end{bmatrix}.$$

Now we can express the CE MIMO-OFDM problem, in a form that can be solved using the GN method for underdetermined nonlinear least squares [25], as

$$(\mathcal{P}_4): \quad \min_{\mathbf{v}\in\mathbb{R}^{MN+1}} f(\mathbf{v}) \colon = \frac{1}{2}\sum_{i=1}^{2KN} \mathbf{r}_i(\mathbf{v})^2 = \frac{1}{2}||\mathbf{r}(\mathbf{v})||_2^2. \tag{32}$$

GN is an alternation of the Newton's method where we use an approximation of the Hessian that does not require information about the second order derivative. In Newton's method in order to find the search direction $\mathbf{p}_N$ we must solve the system $\nabla^2 f(\mathbf{v})\mathbf{p}_N = -\nabla f(\mathbf{x})$. In GN we approximate the Hessian as

$$\nabla^2 f(\mathbf{v}) \approx \mathbf{J}_r^T\mathbf{J}_r, \tag{33}$$

where $\mathbf{J}_r$ is the Jacobian matrix with its (i,j)-element defined as

$$\mathbf{J}_{\mathbf{r}ij} = \frac{\partial r_i(\mathbf{v})}{\partial \mathbf{v}_j}. \tag{34}$$

We arrive at the approximation (33) if we set $\mathbf{D}(\mathbf{v}) = \sum_{i=1}^{2KN} r_i(\mathbf{v})\nabla^2 r_i(\mathbf{v})$ to zero, since $\nabla^2 f(\mathbf{v}) = \mathbf{J}_r^T\mathbf{J}_r + \mathbf{D}(\mathbf{v})$. The approximation $\mathbf{D}(\mathbf{v}) = 0$ is valid either when $\mathbf{v}$ is close to the optimal solution $\mathbf{v}_{opt}$ because the residuals $\mathbf{r}$ there are close to affine [24] (therefore $\nabla^2 r_i(\mathbf{v})$ is relatively small) or $\mathbf{v}$ leads to small residuals ($r_i(\mathbf{v})$ is relatively small). As a consequence, in order for the assumption to be valid and for the algorithm to quickly converge we need to initialize it with a $\mathbf{v}$ that results to a small residual $\mathbf{r}(\mathbf{v})$.

As a result, in order to obtain the search direction $\mathbf{p}_{GN}$ of GN we must solve

$$\mathbf{J}_r^T\mathbf{J}_r\mathbf{p}_{GN} = -\mathbf{J}_r^T\mathbf{r}(\mathbf{v}). \tag{35}$$

Finally, by solving the system above [25], we derive the update step for the $j+1$-th iteration of the method which is

$$\mathbf{v}^{(j+1)} = \mathbf{v}^{(j)} - \mathbf{J_r}^T(\mathbf{J_r}\mathbf{J_r}^T)^{-1}\mathbf{r}(\mathbf{v}^{(j)}). \tag{36}$$

Let us now take a closer look at the details of the implementation of the proposed algorithm, shown in pseudocode in Algorithm 2. For the first step of the algorithm, which is to initialize $\mathbf{v}^{(0)} = [\tilde{\theta}^{(0)T}\beta^{(0)}]^T$, we compute the Zero Forcing precoding vector as

$$\tilde{\mathbf{x}}_{TZF} = \tilde{\mathbf{Q}}^H(\tilde{\mathbf{Q}}\tilde{\mathbf{Q}}^H)^{-1}\tilde{\mathbf{s}} \tag{37}$$

and we calculate the initial angles as $\tilde{\theta}^{(\mathbf{0})} = \text{Arg}(\tilde{\mathbf{x}}_{TZF})$ and the initial $\beta^{(0)}$ as in (25). Next, the j-th, with $j = 1, 2, \ldots, maxIter$ iteration of the algorithm begins by computing the residuals as

$$\mathbf{r}(\mathbf{v}^{(\mathbf{j-1})}) = \begin{bmatrix} \Re\{\tilde{\mathbf{s}} - \beta^{(j-1)}\tilde{\mathbf{Q}}\frac{e^{\imath\tilde{\theta}^{(\mathbf{j-1})}}}{\sqrt{M}}\} \\ \Im\{\tilde{\mathbf{s}} - \beta^{(j-1)}\tilde{\mathbf{Q}}\frac{e^{\imath\tilde{\theta}^{(\mathbf{j-1})}}}{\sqrt{M}}\} \end{bmatrix}. \tag{38}$$

After that, we construct the Jacobian $\mathbf{J}_r(\mathbf{v}^{(j-1)})$ with the following way

1) we create a $KN \times MN$ matrix $\mathbf{\Theta}$ by repeating KN times the vector $[\tilde{\theta}^{(j-1)}]^T$
2) we compute the element wise multiplication $\mathbf{A} = \left[\imath\beta\tilde{\mathbf{Q}}. * \frac{e^{\imath\mathbf{\Theta}}}{\sqrt{M}}\right]$
3) we compute the multiplication $\mathbf{B} = \tilde{\mathbf{Q}}\frac{e^{\imath\tilde{\theta}^{(j-1)}}}{\sqrt{M}}$
4) Finally, we get $\mathbf{J}_r$ as

$$\mathbf{J}_r(\mathbf{v}^{(j-1)}) = -\begin{bmatrix}\Re\{[\mathbf{A}\ \mathbf{B}]\} \\ \Im\{[\mathbf{A}\ \mathbf{B}]\}\end{bmatrix} \tag{39}$$

Each iteration is completed by updating the value of $\mathbf{v}$ according to (36). The algorithm is terminated either when the termination criterion, $\left|\mathbf{v}^{(j)} - \mathbf{v}^{(j-1)}\right| \leq \epsilon$, is met or when the number of maximum iterations, $maxIter$, is reached.

GN method can be improved in order to avoid divergence if the cost function does not decrease in every update step. Since $\mathbf{p}_{GN}$ is a descent direction it is true that $f(\mathbf{v}+\alpha\mathbf{p}_{GN}) < f(\mathbf{v})$ for a sufficiently small $\alpha \in (0,1)$. The update step is changed to accordingly to

$$\mathbf{v}^{(j+1)} = \mathbf{v}^{(j)} - \alpha\mathbf{J_r}^T(\mathbf{J_r}\mathbf{J_r}^T)^{-1}\mathbf{r}(\mathbf{v}^{(j)}). \tag{40}$$

and the value of α can be determined by employing a line search algorithm such as Armijo-line search. In our numerical simulations the algorithm always converged without the need for a step size control and therefore the additional complexity that it would introduce is omitted from the computation of the computational complexity of the algorithm.

Finally, the computational complexity of one iteration of the GN algorithm in FLOPS, using the computation costs found in [34], is given by

$$C_{CE,GN} = 8K^3N^3M + 64K^3N^3 + 12K^2N^2 \tag{41}$$
$$+ 4KN^2M - 2KN - MN, \tag{42}$$

or in big $\mathcal{O}$ notation, $\mathcal{O}(K^3\ N^3\ M)$. It is observed that the proposed algorithm reaches convergence in less than 10 iterations.

IV. Numerical Results

In this section we will present various simulation results of the CE MIMO-OFDM system and we will compare the performance of the two proposed algorithms in this paper as well as the algorithm that was proposed in [2] for single carrier CE precoding in frequency selective channels and was then proposed again in [1] for CE precoding in OFDM

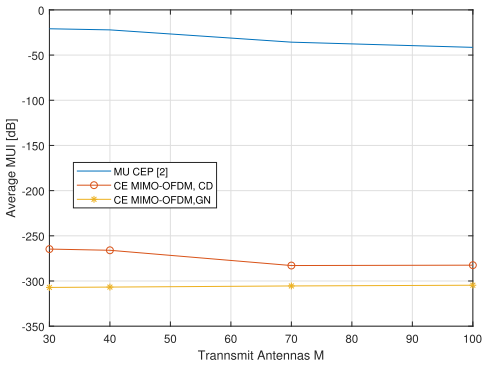

Fig. 3. Average MUI of different CE MIMO-OFDM algorithms for $N = 64$ sub-carriers and $K = 10$ UTs.

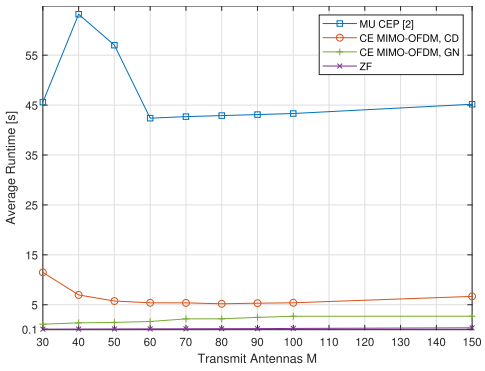

Fig. 4. Average runtime of the different CE MIMO-OFDM algorithms and ZF precoding for $N = 64$ sub-carriers and $K = 10$ UTs.

systems. We will also use as a benchmark scheme the ZF precoder as was described in (37). In the results that follow we have utilized a multipath MIMO channel with $\nu = 8$ resolvable taps, that follow an i.i.d Circularly Symmetric Complex Gaussian distribution with zero mean and variance equal to $1/\nu$, $\mathcal{CN}(0, 1/\nu)$. The PAs are assumed to have unit gain and their input reference amplitude A_{max} is chosen so that for a CE signal of a given amplitude they operate at 1dB backoff. The termination criteria for the algorithms are chosen to be $\epsilon = \epsilon_1 = \epsilon_2 = 10^{-15}$. Additionally, the QAM constellations that are employed are normalized to have average unit power. Finally, in the simulations below β is estimated blindly at the receiver unless it is stated otherwise.

In Fig. 3, we present the average MUI energy, defined as

$$\frac{1}{KN} E_{\tilde{\mathbf{H}}_F, \tilde{\mathbf{x}}_T}[||\tilde{\mathbf{s}} - \beta \tilde{\mathbf{H}}_F \tilde{\mathbf{W}} \tilde{\mathbf{x}}_T||_2^2] \tag{43}$$

of a system with $K = 10$ UTs, $N = 64$ sub-carriers and 16-QAM modulation of the two proposed algorithms for CE MIMO-OFDM in addition to the algorithm presented in [1], [2] for CE precoding over frequency selective channels. The algorithm in the literature rather than transforming the CE problem in the frequency domain as the algorithms in this paper, attempts to find the CE precoding vector in the time domain by calculating the convolution of the channel and the transmit signal at each iteration of the algorithm thus leading to a solution with a higher complexity than the ones proposed here. Additionally, in the competing solution a heuristic splitting of the transmit angles into blocks is performed that can lead to an increased interference. Indeed, we observe that the algorithm for CEP in [2] produces an MUI of about -20 dB when the BS is equipped with 30 transmit antennas and decreases down to about -45 dB as the number of transmit antennas reaches 100. On the other hand, the solutions that we propose here show an excellent performance by reducing the MUI to less than -250 dB even when the number of transmit antennas is 30. This is a result of the efficient proposed model where a heuristic splitting is not necessary, as in [2], and also of the introduction of β which partially compensates for the lack of amplitude control at the transmitter. Finally, we observe that of the two studied algorithms in this paper, the Gauss-Newton solution yields the best results when it comes to reducing the average MUI, as it manages to reach solutions closer to better minima.

Next, in Fig. 4, we compare the average runtime, on a system equipped with an intel core i7 $-$ 8750H CPU, 16 GB RAM and 256 GB SSD, of the GN, CD algorithms as well as the one proposed in [2] for a system with $K = 10$ UTs, $N = 64$ sub-carriers and 16-QAM modulation. We observe that our solutions for CE MIMO-OFDM precoding take significantly less time to converge than the competing algorithm in the literature, and as we have seen from Fig. 3 they also converge to better solutions. The peak in runtime that is observed for the MU CEP when the number of transmit antennas is between 30-50 is due to the fact that the maximum number of iterations is reached without reaching convergence. This shows us that this solution is not suitable when the ratio of UTs to transmit antennas K/M is relatively large. On the other hand, the results show that the most computationally efficient algorithm is the proposed GN as its runtime is less than 5 seconds when $M = 100$ while CD needs about 6 seconds to converge for the same number of transmit antennas. The gap between the two is much larger for a small number of transmit antennas and this is because CD needs a few hundreds of iterations to converge in such scenarios while GN always converges in less than ten iterations. However, as the number of antennas increases the number of iterations for CD decreases almost proportional to $1/(M^2)$ and this justifies the observed average runtime of the algorithm. Finally, the average runtime of ZF precoding for MIMO-OFDM is almost ten times smaller than the runtime of GN ranging from 0.1 seconds when is $M = 30$ to 0.36 seconds when $M = 150$. This gap in computational complexity is expected as ZF precoding does not need an iterative algorithm to run but rather a simple matrix inversion. However, the following results are going to show that CE MIMO-OFDM makes up for the increased complexity with gains in SER performance as well as energy efficiency.

In Fig. 5, we present the SER performance of CE and ZF precoding in MIMO OFDM systems for different output backoff values of the PA. The output backoff (OBO) of an amplifier is given by [21]

$$OBO = 10log\frac{P_o}{P_x} dB, \tag{44}$$

where P_o denotes the maximum output power of the amplifier and P_x is the average output power of the transmitted signal $\mathbf{x}_T$. Additionally the following values have been used for the

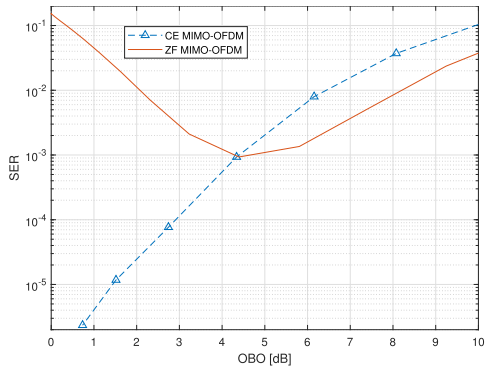

Fig. 5. SER as a function of OBO for a system with $K = 10$ UTs, $M = 50$ BS antennas, $N = 64$ sub-carriers and $16 - QAM$.

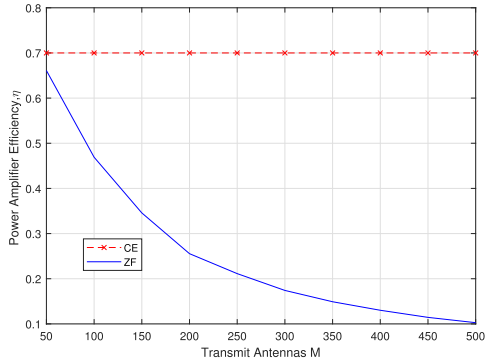

Fig. 6. Average power amplifier efficiency, given by (16), for a system with $M = 100$, $N = 64$, $K = 10$ and 16-QAM.

PAs, $A_{max} = \upsilon = A_{o,max} = 1$ and $p = 2$. We observe that as the OBO decreases the SER performance of CE precoding constantly improves, while on the other hand the performance of ZF precoding reaches its best performance at $4.2dB$ OBO and after that it deteriorates significantly. In order to decrease the OBO of a given PA the average power of the transmit signal $\mathbf{x}_T$ has to be increased. By doing so we also increase the value of the envelope of the signal A. Increasing the envelope of the signal results to significant nonlinear effects which are modelled by the denominator in Eq. (13). Therefore the increase of transmit power which leads to the decrease of OBO drives the PA into its nonlinear region. This induces significant harm to the ZF signal but does not affect the CE signal.

In Fig. 6, we compare the average power amplifier efficiency, given by (16) when CE and ZF precoding is employed. We observe that when CE precoding is used, η remains constant and equal to 0.7 regardless of the number of transmit antennas while when ZF precoding is employed the efficiency falls from about 0.66 to 0.1 as the number of transmit antennas increases from $M = 30$ to $M = 100$. This is the result of the high PAR of the ZF MIMO-OFDM signal and it demonstrates why low PAR techniques such as CE MIMO-OFDM are necessary for large scale antenna systems.

In Fig. 7 the power consumption difference between the architectures for CE MIMO-OFDM and the fully digital architecture for ZF MIMO-OFDM is plotted. The difference between CE and ZF precoding when it comes to power consumption is that the power amplifiers have a different

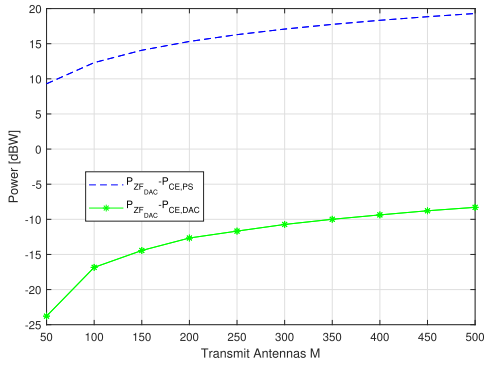

Fig. 7. Power consumption gains of the proposed CE precoding architectures over a fully-digital architecture for ZF precoding, for a system with $M = 100$, $N = 64$, $K = 10$ and 16-QAM.

average power efficiency as we discussed in the previous paragraph. Additionally, as it was mentioned in a previous section CE precoding can be implemented in a system that uses power-efficient PSs instead of DACs. We acquire the plots by assuming the following power consumption values for the components $P_{DAC} = 200$mW, $P_{LO} = 5$mW, $P_{mix} = 19$mW, $P_{fil} = 14$mW, $P_{PS} = 30$mW, [17]– [20] and using the power consumption approximations given by (18) and (19). We observe that both architectures for CE precoding have increasing gains in power consumption over the fully digital architecture for ZF precoding as the number of transmit antennas increases. Additionally, we manage to decrease the power consumption even further by about 30 dBW when using the analog architecture with phase shifters rather than DACs. These results show that these architectures, and especially the analog one, are suitable candidates for large MIMO systems when the objective is to reduce the power consumption.

We will now present the SER performance of different configurations of the two proposed algorithms and we will compare them with the ZF precoder as well as the algorithm that is proposed for CEP in [2] and is used in [1] for OFDM transmission, as shown in Fig. 8. All systems have PAs which operate at the same point in order to have comparable efficiency. The first thing to observe is that the SER performance of the two algorithms is almost identical and so it becomes evident that when taking into account their computational efficiency, as was shown in Fig. 4, the GN algorithm is far more suitable for the CE MIMO-OFDM system. Furthermore, we observe that in both cases when $M = 15$ and $M = 30$ the CE precoding shows better performance than ZF precoding. The bad performance of the ZF precoder and the observed error floor is a result of the in band distortion that is introduced by the non linear power amplifier. On the other hand CE MIMO-OFDM does not suffer from this because of its constant envelope nature. Finally, when compared to prior art CE precoding for OFDM systems [1], [2], the advantage of our system model and algorithmic solutions becomes apparent as it outperforms the prior art scheme by more than $30dB$. This is a result that highlights the importance of the improved formulation which enables efficient algorithmic solutions as well as the different system model which scales the signal at the UTs by β.

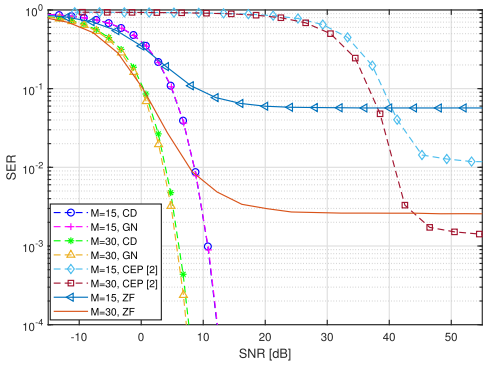

Fig. 8. SER performance of ZF, the two proposed CE MIMO-OFDM algorithms and the algorithm for CEP in [2] for a system with $K = 5$ UTs and $N = 32$ sub-carriers and 16-QAM modulation.

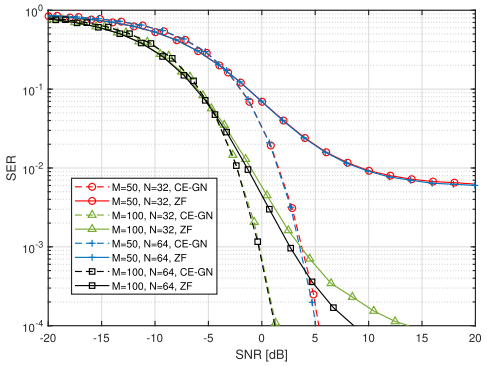

Fig. 9. SER performance of the GN algorithm CE MIMO-OFDM algorithms for a system with $K = 10$ UTs and 16-QAM modulation.

In Fig. 9, we present the SER performance of the GN algorithm for a different number of sub-carriers N and transmit antennas M and we compare with the ZF precoding scheme. Firstly, it is observed that the performance of CE MIMO-OFDM remains identical when we increase the number of sub-carriers from 32 to 64. This is not true for ZF precoding as we observe that when $M = 100$ there is a widening gap between the SER curves that correspond to $N = 64$ and $N = 32$ sub-carriers. The reason for this gap is that a different number of sub-carriers leads to a different PAR in the case of ZF precoding, which results to an increased distortion by non linear amplification. Although, CE MIMO-OFDM precoding performs significantly better than ZF precoding in every scenario it is observed that the performance gap becomes smaller as the number of transmit antennas increases from 50 to 100. However, we should also take into account that as the number of transmit antennas increases the efficiency of the power amplifiers decreases as it was shown in Fig. 6. Therefore, ZF precoding, or any other precoding with high PAR, forces the designer of the system to choose the best trade off between power efficiency and error rate performance, while CE precoding has always high power amplifier efficiency without impeding the performance of the system.

In the figures above while the superiority in SER performance of the proposed CE MIMO-OFDM precoding is clearly shown there is not a clear connection with the power consumption gains of the proposed architecture for CE MIMO-OFDM precoding. To this end we will use the metric of energy

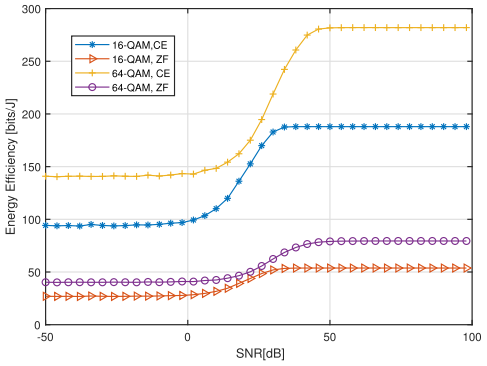

Fig. 10. Energy efficiency of systems equipped with $M = 100$ transmit antennas, $K = 10$ UTs and $N = 32$ subcarriers.

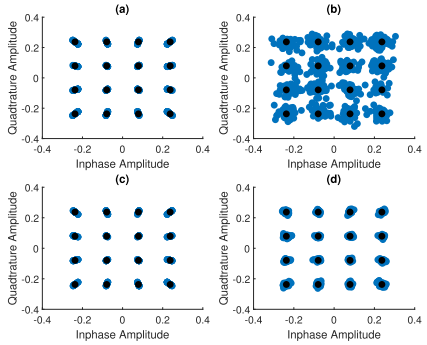

Fig. 11. Received noiseless signal points when transmitting 16-QAM symbols with nonlinear amplification over a MIMO frequency selective channel using $N = 64$ subcarriers (a) CE MIMO-OFDM, $M = 50$, $K = 10$, (b) ZF MIMO-OFDM, $M = 50$, $K = 10$, (c) CE MIMO-OFDM, $M = 100$, $K = 10$, (d) ZF MIMO-OFDM, $M = 100$, $K = 10$.

efficiency as defined in [36],

$$EE(P_{kn}^e, b, K, N) = \frac{\sum_{n=1}^{N}\sum_{k=1}^{K}(1 - P_{kn}^e)b}{P}, \qquad (45)$$

where P_{kn}^e is the bit error probability per UT and per subcarrier, b is the number of bits per constellation symbol and P denotes the power that is consumed by the transmitter and is given by (18) or (19). In Fig. 10 it is shown that the power efficient components that are used by the transmitter of CE MIMO-OFDM result in a significantly better energy efficiency when compared to ZF precoding. What is more, it is proved that CE MIMO-OFDM precoding can employ higher order modulations such as $64 - QAM$ that result in a significantly better rate and overall energy efficiency. On the other hand ZF precoding, does not only have poorer SER performance as it was discussed above, but its overall power consumption drives its energy efficiency down. Finally, the increase of the modulation order to $64 - QAM$ does not yield the same improvement in rate and energy efficiency as it does for CE precoding because of the harm induced by the nonlinear distortion which is becomes more damaging as the modulation order increases.

In order to better showcase the effect of nonlinear amplification, we illustrate in Fig. 11 the received signal points without thermal noise of a CE and ZF MIMO-OFDM system. It is observed that for the CE system the distortion variance is very small regardless of the number of transmit antennas

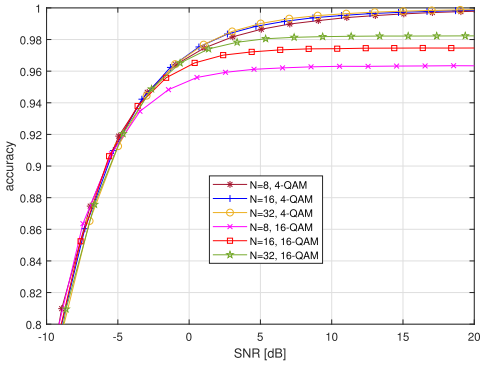

Fig. 12. Accuracy of the estimated $\hat{\beta}_k$ as a function of the SNR for a system with $M = 30$ transmit antennas and $K = 5$ UTs.

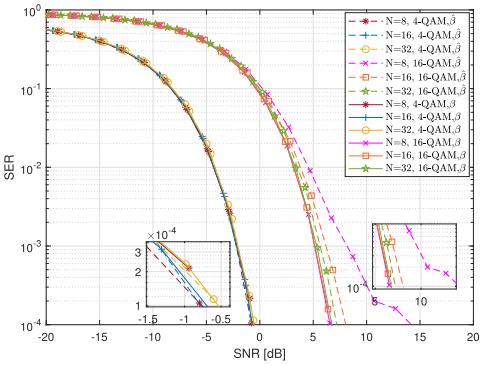

Fig. 13. SER performance comparison of the proposed CE MIMO-OFDM for the cases of perfect knowledge of β and blind estimation of $\hat{\beta}_k$, in a system with $M = 30$ transmit antennas and $K = 5$ UTs.

and as we have seen in the previous figures it does not affect negatively the SER performance. On the other hand, when ZF precoding is employed the distortion variance is very significant, especially when the number of transmit antennas is $M = 50$ which explains why we observed an error floor in the previous figures. As the number of transmit antennas increases to $M = 100$ the distortion variance decreases but so does the efficiency of the amplifier as we showed in Fig. 6.

In the last two figures, we will see the accuracy of the $\hat{\beta}_k$ blind estimation at the UTs and the effect that the different number of sub-carriers and modulation order have on its estimation and the overall performance of the system. In Fig. 12 we show the accuracy of $\hat{\beta}_k$ as a function of the SNR when $4 - QAM$ and $16 - QAM$ modulation is employed. The accuracy is defined as

$$\text{accuracy} = 1 - \frac{\hat{\beta}_k - \beta}{\beta}. \tag{46}$$

We observe that as expected the accuracy of the estimation is improved as the SNR increases. The rate of the increase is dependent on the employed modulation and the length of the OFDM block. For example when 16-QAM is used in an OFDM block of 32 sub-carriers the accuracy of the estimation is 98% for an SNR value of 5dB while the accuracy drops to 96% for the same SNR when the OFDM block has only 8 sub-carriers. Furthermore, we observe that for the higher order modulation the accuracy stops increasing with the SNR after some point, thus creating the need for either using larger OFDM-blocks or inserting pilots to estimate β. In Fig. 13 we compare the SER of a system that has perfect knowledge of β and one that estimates it blindly according to (12). We observe that when 4-QAM is used the SER of the systems that have perfect knowledge of β have identical SER performance with those that estimate it no matter the size of the OFDM block. However, for 16-QAM if the size of the OFDM block is relatively small we see that there is a gap between the system with perfect knowledge and the one with the blind estimate of β, which increases as the OFDM block size becomes smaller. This was expected, as we observed from the previous figure that the estimation accuracy took a hit when 16-QAM modulation and small OFDM blocks were used. Therefore, while β is a strong point of the proposed system that makes our algorithm converge faster to a solution and takes into account the array gain, it also introduces some trade-offs that have to be made during the implementation. If large OFDM blocks are used, as in most practical applications, then we can use high order modulations without degrading the system performance. If on the other hand we have to use smaller OFDM blocks we either have to use lower order modulations to avoid performance degradation due to estimation error or introduce pilot symbols in order to improve the estimation of β.

V. Conclusion

In this paper we addressed the per antenna CE precoding in a MIMO-OFDM system. We employed a system model that helps us design the time domain CE precoder in the frequency domain in order to avoid using the computationally complex convolution. We achieved that by reformulating the channel matrix and the DFT matrix and we managed to formulate a least-squares problem with a constant modulus constraint. Additionally, we introduced the factor β which changes per OFDM block and is estimated blindly at the UTs where it is used to rescale the received signal.

First, we solved the problem by using a CD based algorithm. However, the per iteration complexity of the solution increased rapidly with the number of transmit antennas.

For this reason, we developed a more efficient solution based on the GN method. To solve it using GN we had to reformulate it first into a nonlinear least-squares problem. The solution proved to be very efficient and achieved improvements both in runtime and minimizing the MUI, when compared to similar solutions in the literature and our proposed CD based algorithm.

We also showed that the SER performance of the two proposed solutions is identical and outperforms ZF precoding which was used as a benchmark. Furthermore, because of the power consumption gains that are derived from the implementation of the transmitter architecture for CE precoding with efficient non linear power amplifiers and analog phase shifters rather than DACs, the proposed CE MIMO-OFDM precoding scheme and transmitter architecture is an excellent candidate for large scale antenna systems. Finally, we also discussed the considerations that have to be made so that the estimation of β will not affect the system performance and showed that for systems with a large OFDM block the estimation of β should not affect the performance.

REFERENCES

[1] C. Mollen, E. G. Larsson, and T. Eriksson, "Waveforms for the massive MIMO downlink: Amplifier efficiency, distortion, and performance," *IEEE Trans. Commun.*, vol. 64, no. 12, pp. 5050–5063, Dec. 2016.

[2] S. K. Mohammed and E. G. Larsson, "Constant-envelope multi-user precoding for frequency-selective massive MIMO systems," *IEEE Wireless Commun. Lett.*, vol. 2, no. 5, pp. 547–550, Oct. 2013.

[3] F. Rusek, D. Persson, B. Kiong Lau, E. G. Larsson, T. L. Marzetta, and F. Tufvesson, "Scaling up MIMO: Opportunities and challenges with very large arrays," *IEEE Signal Process. Mag.*, vol. 30, no. 1, pp. 40–60, Jan. 2013.

[4] E. G. Larsson, O. Edfors, F. Tufvesson, and T. L. Marzetta, "Massive MIMO for next generation wireless systems," *IEEE Commun. Mag.*, vol. 52, no. 2, pp. 186–195, Feb. 2014.

[5] H. Quoc Ngo, E. G. Larsson, and T. L. Marzetta, "Energy and spectral efficiency of very large multiuser MIMO systems," *IEEE Trans. Commun.*, vol. 61, no. 4, pp. 1436–1449, Apr. 2013.

[6] M. Alodeh *et al.*, "Symbol-level and multicast precoding for multiuser multiantenna downlink: A state-of-the-art, classification, and challenges," *IEEE Commun. Surveys Tuts.*, vol. 20, no. 3, pp. 1733–1757, 3rd Quart., 2018.

[7] M. Alodeh, S. Chatzinotas, and B. Ottersten, "A multicast approach for constructive interference precoding in MISO downlink channel," in *Proc. IEEE Int. Symp. Inf. Theory*, Jun. 2014, pp. 2534–2538.

[8] V. R. Cadambe and S. Ali Jafar, "Interference alignment and degrees of freedom of the K-user interference channel," *IEEE Trans. Inf. Theory*, vol. 54, no. 8, pp. 3425–3441, Aug. 2008.

[9] M. A. Maddah-Ali, A. S. Motahari, and A. K. Khandani, "Communication over MIMO x channels: Interference alignment, decomposition, and performance analysis," *IEEE Trans. Inf. Theory*, vol. 54, no. 8, pp. 3457–3470, Aug. 2008.

[10] C. Masouros and G. Zheng, "Exploiting known interference as green signal power for downlink beamforming optimization," *IEEE Trans. Signal Process.*, vol. 63, no. 14, pp. 3628–3640, Jul. 2015.

[11] P. V. Amadori and C. Masouros, "Large scale antenna selection and precoding for interference exploitation," *IEEE Trans. Commun.*, vol. 65, no. 10, pp. 4529–4542, Oct. 2017.

[12] A. Kalantari, C. Tsinos, M. Soltanalian, S. Chatzinotas, W.-K. Ma, and B. Ottersten, "MIMO directional modulation M-QAM precoding for transceivers performance enhancement," in *Proc. IEEE 18th Int. Workshop Signal Process. Adv. Wireless Commun. (SPAWC)*, Jul. 2017, pp. 1–5.

[13] M. Bengtsson and B. Ottersten, "Optimal and suboptimal transmit beamforming," in *Handbook of Antennas in Wireless Communications*, L. C. Godara, Ed. Boca Raton, FL, USA: CRC Press, 2001.

[14] M. Schubert and H. Boche, "Solution of the multiuser downlink beamforming problem with individual SINR constraints," *IEEE Trans. Veh. Technol.*, vol. 53, no. 1, pp. 18–28, Jan. 2004.

[15] Q. H. Spencer, A. L. Swindlehurst, and M. Haardt, "Zero-forcing methods for downlink spatial multiplexing in multiuser MIMO channels," *IEEE Trans. Signal Process.*, vol. 52, no. 2, pp. 461–471, Feb. 2004.

[16] S. Jacobsson, G. Durisi, M. Coldrey, T. Goldstein, and C. Studer, "Quantized precoding for massive MU-MIMO," *IEEE Trans. Commun.*, vol. 65, no. 11, pp. 4670–4684, Nov. 2017.

[17] C. G. Tsinos, S. Maleki, S. Chatzinotas, and B. Ottersten, "On the energy-efficiency of hybrid analog–digital transceivers for Single- and multi-carrier large antenna array systems," *IEEE J. Sel. Areas Commun.*, vol. 35, no. 9, pp. 1980–1995, Sep. 2017.

[18] R. Mendez-Rial, C. Rusu, N. Gonzalez-Prelcic, A. Alkhateeb, and R. W. Heath, "Hybrid MIMO architectures for millimeter wave communications: Phase shifters or switches?" *IEEE Access*, vol. 4, pp. 247–267, 2016.

[19] S. Cui, A. J. Goldsmith, and A. Bahai, "Energy-constrained modulation optimization," *IEEE Trans. Wireless Commun.*, vol. 4, no. 5, pp. 2349–2360, Sep. 2005.

[20] S. Domouchtsidis, C. G. Tsinos, S. Chatzinotas, and B. Ottersten, "Symbol-level precoding for low complexity transmitter architectures in large-scale antenna array systems," *IEEE Trans. Wireless Commun.*, vol. 18, no. 2, pp. 852–863, Feb. 2019.

[21] C. Rapp, "Effects of HPA-nonlinearity on 4-DPSK/OFDM-signal for a digital sound broadcasting system," in *Proc. 2nd Eur. Conf. Satellite Commun.*, 1991, pp. 179–184.

[22] S. C. Cripps, *RF Power Amplifiers for Wireless Communications*. Norwood, MA, USA: Artech House, 1999.

[23] D. P. Bertsekas, *Nonlinear Programming*. Belmont, MA, USA: Athena Scientific, 1999.

[24] J. Nocedal and S. Wright, *Numerical Optimization* (Springer Series in Operations Research and Financial Engineering), 2nd ed. Cham, Switzerland: Springer, 2006.

[25] J.-F. Bao, C. Li, W.-P. Shen, J.-C. Yao, and S.-M. Guu, "Approximate Gauss–Newton methods for solving underdetermined nonlinear least squares problems," *Appl. Numer. Math.*, vol. 111, pp. 92–110, Jan. 2017.

[26] S. K. Mohammed and E. G. Larsson, "Single-user beamforming in large-scale MISO systems with per-antenna constant-envelope constraints: The doughnut channel," *IEEE Trans. Wireless Commun.*, vol. 11, no. 11, pp. 3992–4005, Nov. 2012.

[27] S. K. Mohammed and E. G. Larsson, "Per-antenna constant envelope precoding for large multi-user MIMO systems," *IEEE Trans. Commun.*, vol. 61, no. 3, pp. 1059–1071, Mar. 2013.

[28] J.-C. Chen, C.-K. Wen, and K.-K. Wong, "Improved constant envelope multiuser precoding for massive MIMO systems," *IEEE Commun. Lett.*, vol. 18, no. 8, pp. 1311–1314, Aug. 2014.

[29] F. Liu, C. Masouros, P. V. Amadori, and H. Sun, "An efficient manifold algorithm for constructive interference based constant envelope precoding," *IEEE Signal Process. Lett.*, vol. 24, no. 10, pp. 1542–1546, Oct. 2017.

[30] S. Zhang, R. Zhang, and T. J. Lim, "Constant envelope precoding for MIMO systems," *IEEE Trans. Commun.*, vol. 66, no. 1, pp. 149–162, Jan. 2018.

[31] N. Prasad, X.-F. Qi, and A. Gatherer, "Optimizing beams and bits: A novel approach for massive MIMO base-station design," in *Proc. Int. Conf. Comput., Netw. Commun. (ICNC)*, Feb. 2019, pp. 970–976.

[32] A. Goldsmith, *Wireless Communications*. Cambridge, U.K.: Cambridge Univ. Press, 2005.

[33] S. Haykin, *Communication Systems*, 4th ed. Hoboken, NJ, USA: Wiley, 2001.

[34] R. Hunger, *Floating Point Operations in Matrix-Vector Calculus*. Munich, Germany: Munich Univ. of Technology, Inst. for Circuit Theory and Signal Processing Munich, 2007.

[35] S. Domouchtsidis, C. Tsinos, S. Chatzinotas, and B. Ottersten, "Constant envelope massive MIMO-OFDM precoding: An improved formulation and solution," in *Proc. IEEE Int. Conf. Acoust., Speech Signal Process. (ICASSP)*, May 2020, pp. 8956–8960.

[36] S. Payami, M. Ghoraishi, M. Dianati, and M. Sellathurai, "Hybrid beamforming with a reduced number of phase shifters for massive MIMO systems," *IEEE Trans. Veh. Technol.*, vol. 67, no. 6, pp. 4843–4851, Jun. 2018.

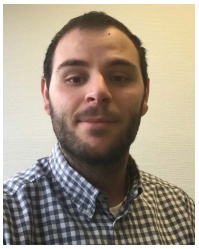

Stavros Domouchtsidis (Student Member, IEEE) was born in Lamia, Greece, in 1992. He received the M.Eng. degree in electrical and computer engineering from the Aristotle University of Thessaloniki, Greece, in 2016, and the Ph.D. degree in informatics from the University of Luxembourg, Luxembourg. He is currently a Post-Doctoral Research Scientist with the Interdisciplinary Centre for Security, Reliability, and Trust, University of Luxembourg. His current research interests include signal processing for mmWave, massive MIMO, and satellite communications.

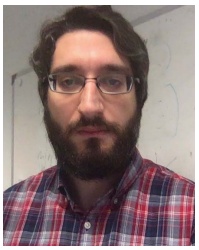

Christos G. Tsinos (Senior Member, IEEE) received the Diploma degree in computer engineering and informatics, the M.Sc. and Ph.D. degrees in signal processing and communication systems, and the M.Sc. degree in applied mathematics from the University of Patras, Greece, in 2006, 2008, 2013, and 2014, respectively. From 2014 to 2015, he was a Post-Doctoral Researcher with the University of Patras. In 2015, he joined the Interdisciplinary Centre for Security, Reliability, and Trust (SnT), University of Luxembourg, Luxembourg. In the past, he was involved in a number of different Research and Development projects funded by national and/or EU funds. He is currently the Principal Investigator of Research and Development Project Energy and Complexity Efficient Millimeter-Wave Large-Array Communications (ECLECTIC), funded by the FNR CORE Framework. His current research interests include optimization and machine learning for signal processing and communications. He is a member of the Technical Chamber of Greece.

Symeon Chatzinotas (Senior Member, IEEE) received the M.Eng. degree in telecommunications from the Aristotle University of Thessaloniki, Thessaloniki, Greece, in 2003, and the M.Sc. and Ph.D. degrees in electronics engineering from the University of Surrey, Surrey, U.K., in 2006 and 2009, respectively. He was involved in numerous research and development projects with the Institute of Informatics Telecommunications, National Centre of Scientific Research Demokritos, the Institute of Telematics and Informatics, the Center of Research and Technology Hellas, and the Mobile Communications Research Group, Center of Communication Systems Research, University of Surrey. He is currently the Deputy Head of the SIGCOM Research Group, Interdisciplinary Centre for Security, Reliability, and Trust, University of Luxembourg, Luxembourg, and a Visiting Professor with the University of Parma, Italy. He has over 300 publications, 3000 citations, and an H-index of 30 according to Google Scholar. He was a Corecipient of the IEEE Distinguished Contributions to Satellite Communications Award in 2014, the CROWNCOM Best Paper Award in 2015, and the EURASIP JWCN Best Paper Award in 2018.

Björn Ottersten (Fellow, IEEE) was born in Stockholm, Sweden, in 1961. He received the M.S. degree in electrical engineering and applied physics from Linköping University, Linköping, Sweden, in 1986, and the Ph.D. degree in electrical engineering from Stanford University, Stanford, CA, USA, in 1990.

He has held research positions with the Department of Electrical Engineering, Linköping University, the Information Systems Laboratory, Stanford University, Katholieke Universiteit Leuven, Leuven, Belgium, and the University of Luxembourg, Luxembourg. From 1996 to 1997, he was the Director of research with ArrayComm Inc., a start-up in San Jose, CA, USA, based on his patented technology. In 1991, he was appointed as a Professor of signal processing at the Royal Institute of Technology (KTH), Stockholm, where he was the Head of the Department of Signals, Sensors, and Systems, from 1992 to 2004. From 2004 to 2008, he was the Dean of the School of Electrical Engineering, KTH. He is currently the Director of the Interdisciplinary Centre for Security, Reliability, and Trust, University of Luxembourg. As the Digital Champion of Luxembourg, he acts as an Adviser of the European Commission. He is a fellow of the EURASIP. He was a recipient of the EURASIP Meritorious Service Award in 2010, the European Research Council Advanced Research Grant from 2009 to 2013, and the IEEE Signal Processing Society Technical Achievement Award in 2011. He will receive the European Research Council Advanced Research Grant. He has coauthored journal articles that received the IEEE Signal Processing Society Best Paper Award in 1993, 2001, 2006, and 2013, and seven other IEEE conference papers best paper awards. He has served as the Editor-in-Chief for the *EURASIP Signal Processing Journal* and an Associate Editor for the IEEE TRANSACTIONS ON SIGNAL PROCESSING, and served on the Editorial Board of the *IEEE Signal Processing Magazine*. He is currently a member of the Editorial Boards of the *EURASIP Signal Processing Journal*, the *EURASIP Journal of Advances in Signal Processing*, and the *Foundations and Trends of Signal Processing*.